

Optimized Power Allocation and Signal Shaping for Interference-Limited Multi-antenna “Ad Hoc” Networks

Enzo Baccarelli and Mauro Biagi

INFO-COM Dept., University of Rome,
via Eudossiana 18, 00184, Rome (Italy)

FAX no. +39 (0)64873300

enzobac@infocom.uniroma1.it

Phone.no. +39 (0)644585466

m.biagi@ieee.org

Phone.no. +39 (0)644585471

Abstract. This paper deals with optimized Multiple-Input Multiple Output (MIMO) channel estimation and ensuing information throughput conveyed by pilot-based multi-antenna systems affected by both spatially colored Multiple Access Interference (MUI) and *errors* in the available channel estimates. The architecture of the Minimum Mean Square Error (MMSE) MIMO channel estimator is derived and the related analytical conditions for the optimal design of space-time training sequences are provided. Afterwards, closed form expressions for the maximum information throughput sustained by the considered systems for Gaussian distributed input signals are given and, then, a novel powers' allocation algorithm for the asymptotical achievement of the system capacity is developed. Considerations about optimized space-division MAC strategies are also provided.

1 Introduction and Goals

Due to fast increasing demand lastly experienced for pervasive high-throughput Wireless “ad-hoc” LANs, Multi-Antenna systems seem to be adequate as innovative technological approach to guarantee reliable performance and also power saving. In this context, we propose an innovative algorithm for power allocation in Rayleigh flat fading environment for Multi-Antenna transceiver so to exploit spatial diversity in order to maximize mutual information also in the presence of Multi Access interference. The transmission scheme we based on is continuous and does not required orthogonal access (e.g. orthogonal TDMA, FDMA or CDMA). Therefore, in this work we focus on the ultimate information throughput conveyed by pilot-based wireless MIMO systems equipped with *imperfect* channel estimates at both transmit and receiver and impaired by *spatially colored MUI*. Specifically, main contributions of this work may be summarized as follows. First, we develop the optimal MMSE channel estimator for pilot-based MIMO systems impaired by colored MUI. Second, we provide the analytical

properties characterizing optimized space-time training sequences and then we show as these last are related to the statistics of spatial MUI. Third, we develop closed-form analytical expressions for computing the information throughput sustained by considered MIMO system for the case of Gaussian distributed input signals and then we point out several asymptotical operating conditions guaranteeing achievement of the corresponding system capacity. Fourth, we propose an iterative algorithm for the optimized power allocation when *imperfect* channel estimates are available at both transmit/receiver. Before proceeding few words about the adopted notation. Capital letters indicate matrices, lower-case underlined symbols denote vectors while characters overlined by arrow \rightarrow denote block-matrices and block-vectors. Apexes $*$, T , † mean conjugation, transposition and conjugate-transposition respectively while lower-case letters will be used for scalar quantities. Again, $\det[A]$ and $\text{Tra}[A]$ mean determinant and trace of matrix $A \doteq [\underline{a}_1 \dots \underline{a}_m]$, while $\text{vect}(A)$ indicates the (block) vector obtained by the ordered stacking of the column of matrix A. Finally, I_m is the (mxm) unit matrix, $\|A\|_E$ is the Euclidean norm of matrix A, $A \otimes B$ is the Kronecker product of matrix A by matrix B, $\underline{0}_m$ is the m-dimensional zero-vector, \lg denotes natural logarithm and $\delta(m, n)$ is the Kroenecker delta.

2 System Modeling

The considered application scenario is that of emerging local wireless “ad-hoc” networks [18,20] where a (large) number of uncoordinated transmit-receiving nodes simultaneously communicate over a limited hot-spot cell and then give arise to mutual multiple access interference [18]. Simply stated, it is composed by a transmitter unit equipped with $t \geq 1$ antennas communicating to a receiving unit equipped with $r \geq 1$ antennas via a radio channel impaired by both slow-variant flat Rayleigh fading and additive multiple access interference induced by adjacent nodes active over the same hot-spot cell. Path gain h_{ji} from transmitter antenna i to receiver on j may be modelled as a complex zero-mean unit-variance proper complex variable (r.v.) [5,6,7,8] and, for sufficiently spaced apart antennas, these path gains $\{h_{ji} \in \mathbb{C}^1, 1 \leq j \leq r, 1 \leq i \leq t\}$ may be considered¹ uncorrelated. Furthermore, for low-mobility applications as those serving nomadic users over hot-spot cells, path gains $\{h_{ji}\}$ may be also assumed time-invariant over $T \geq 1$ signalling periods, after which they change to new *statistically independent* values held for another T signalling periods and so on. We assume that the coded and modulated streams radiated by transmitter antennas are split into packets composed by $T \geq 1$ slots, where first $T_L \geq 0$ slots are used by Rx for learning the MUI statistics (See Sect.II.1), second $T_{tr} \geq 0$ slots are employed for estimating the path gains $\{h_{ji}\}$ of the forward MIMO channel (see Sect.II.2) and, finally, last $T_{pay} \triangleq T - T_{tr} - T_L$ slots convey payload data (see Sect.II.3). Thus, after indicating as R_C (nats/slot) the information rate of

¹ For hot-spot local area applications, antenna spacing of the order of $\lambda/2$ suffices for meeting the above assumption [15].

the employed space-time encoder, the spectral efficiency η (nats/sec/Hz) of the described system equates

$$\eta = \frac{T_{pay}}{T} \cdot \frac{R_C}{\Delta_s B_w}, \quad (1)$$

where Δ_s (sec.) and B_w are slot duration and RF bandwidth of radiated signal, respectively.

2.1 Learning Phase

During the learning phase, no signals are radiated by transmitter Tx so to allow corresponding receiver Rx to learn statistics of the impairing MUI. More in particular, the r -dimensional (complex column) vector $\underline{y}(n) \triangleq [\underline{y}_1(n) \dots \underline{y}_r(n)]^T$ collecting the outputs of the r receiving antennas over the n -th slot of the learning phase may be modeled as

$$\underline{y}(n) \triangleq \underline{d}(n) \equiv \underline{v}(n) + \underline{w}(n). \quad (2)$$

The first component accounts for the receiver thermal noise and then $\{\underline{w}(n) \in \mathbb{C}^r, 1 \leq n \leq T_L\}$ may be modeled as a zero-mean, proper complex, spatially correlated and temporally white, Gaussian sequence with covariance matrix equal to

$$E\{\underline{w}(n)(\underline{w}(m))^\dagger\} = N_0 \mathbf{I}_r \delta(m, n) \quad (3)$$

where N_0 (watt/Hz) is the level of the receiving thermal noise. Since the second component $\{\underline{v}(n)\}$ in (2) accounts for the MUI due to multiple co-located transmitting nodes active over the same hot-spot cell, it is likelihood to model $\{\underline{v}(n) \in \mathbb{C}^r\}$ as a zero-mean temporally white, spatially colored proper Gaussian sequence, whose covariance matrix

$$\mathbf{K}_v \triangleq E\{\underline{v}(n)(\underline{v}(m))^\dagger\} \equiv \begin{bmatrix} c_{11} & \dots & c_{1r} \\ c_{12}^* & \dots & c_{2r} \\ \vdots & \vdots & \vdots \\ c_{1r}^* & \dots & c_{rr} \end{bmatrix} \quad (4)$$

remains unchanged over time intervals at least equal to the duration of an overall packet. However, this last may change from a packet to another so that it is reasonable to assume that both Tx and Rx nodes are not aware of the covariance matrix of the overall disturbance:

$$\mathbf{K}_d \triangleq E\{\underline{d}(n)(\underline{d}(m))^\dagger\} \equiv \mathbf{K}_v + N_0 \mathbf{I}_r, \quad (5)$$

at the beginning of each transmitted packet. However, since the received signals $\{\underline{y}(n)\}$ equate the MAI ones $\{\underline{f}(n)\}$ during the learning phase, laws of large numbers guarantees that an unbiased and consistent (e.g, asymptotically exact)

estimate $\overset{\vee}{K}_d$ of the (a priori) unknown covariance matrix K_d is given by the following relationship:

$$\overset{\vee}{K}_d = \frac{1}{T_L} \sum_{n=1}^{T_L} \underline{\dot{y}}(n)(\underline{\dot{y}}(n))^\dagger. \quad (6)$$

2.2 Training Phase

On the basis of the allowable MUI covariance matrix K_d , during the training phase the Tx transmitter node is able to perform the optimized shaping of the deterministic pilot streams $\{\tilde{x}_i(n) \in \mathbb{C}^1, T_L + 1 \leq n \leq T_L + T_{tr}\}, 1 \leq i \leq t$, to be used for estimating the (a priori unknown) path gains $\{h_{ji}\}$ of the MIMO (forward) channel. In particular, the (Δ_s -sampled) signals $\{\tilde{y}_j(n) \in \mathbb{C}^1, T_L + 1 \leq n \leq T_L + T_{tr}\}, 1 \leq j \leq r$, measured at the output of j -th receiving antenna during the training phase may be modelled as

$$\tilde{y}_j(n) = \frac{1}{\sqrt{t}} \sum_{i=1}^t h_{ji} \tilde{x}_i(n) + \tilde{d}_j(n), \quad T_L + 1 \leq n \leq T_L + T_{tr}, 1 \leq j \leq r, \quad (7)$$

where the corresponding overall disturbance

$$\tilde{d}_j(n) = \tilde{v}_j(n) + \tilde{w}_j(n), \quad T_L + 1 \leq n \leq T_L + T_{tr}, 1 \leq j \leq r, \quad (7.1)$$

is independent from path gains $\{h_{ji}\}$ and exhibits the *same* statistics previously detailed in (4), (5) for the learning phase. Thus, after assuming the (usual) constraint

$$\frac{1}{t} \sum_{i=1}^t \|\tilde{x}_i(n)\|^2 = \tilde{P}, \quad T_L + 1 \leq n \leq T_L + T_{tr}, \quad (8)$$

about the average power \tilde{P} radiated by transmitting antennas over each slot of the training phase, the corresponding signal to interference-plus-noise ratio (SINR) $\tilde{\gamma}_j$ measured at the output of j -th receiving antennas equates (see eqs.(7), (8))

$$\tilde{\gamma}_j = \tilde{P}/(N_0 + c_{jj}), \quad 1 \leq j \leq r \quad (8.1)$$

where $N_0 + c_{jj}$ is the j -th diagonal entry of the MUI matrix K_d in (5). Therefore, the T_{tr} -xr (complex) samples gathered at the outputs of the r receive antennas during overall training phase may be organized into the (T_{tr}, xr) observed matrix $\tilde{Y} \triangleq [\tilde{y}_1 \dots \tilde{y}_r]$ given by [6,7]

$$\tilde{Y} = \frac{1}{\sqrt{t}} \tilde{X} H + \tilde{D}, \quad (9)$$

where $\tilde{X} \triangleq [\tilde{x}_1 \dots \tilde{x}_t]$ is the (T_{tr}, xt) matrix of (deterministic) pilot symbols, $H \triangleq [h_1 \dots h_r]$ is the (txr) complex matrix composed by path gains $\{h_{ji}\}$ and the

(T_{tr} xr) matrix $\tilde{D} \triangleq [\tilde{d}_1 \dots \tilde{d}_r]$ collects the disturbance samples $\{\tilde{d}_j(n)\}$ in (7) experienced during the training phase. Obviously, from (8) it follows that the pilot matrix \tilde{X} in (9) must satisfy the following second order constraint:

$$Tra[\tilde{X}\tilde{X}^\dagger] = tT_{tr}\tilde{P}. \tag{9.1}$$

As detailed in Sect.III, training observations in (9) are employed by the receiver node Rx for computing the MMSE matrix estimate $\hat{H} \triangleq E\{H\tilde{Y}\}$ of the MIMO channel H. In turn, at step $n = T_L + T_{tr}$ (e.g., at the end of training phase) this estimates \hat{H} are communicated back to the transmitter via an (ideal) feedback link.

2.3 Payload Phase

Thus, on the basis of available K_d and \hat{H} matrices and actual message \mathfrak{M} to be communicated, the transmitting Tx node suitably shapes the (random) signal streams $\{\phi_i(n) \in \mathbb{C}^1, T_L + T_{tr} + 1 \leq n \leq T\}$, $1 \leq i \leq t$, to be radiated by t transmitting antennas during the payload phase. The corresponding (sampled) signals $\{y_j(n) \in \mathbb{C}^1, T_L + T_{tr} + 1 \leq n \leq T\}$, $1 \leq j \leq r$ measured at the outputs of r receiving antennas may be modelled as

$$y_j(n) = \frac{1}{\sqrt{t}} \sum_{i=1}^t h_{ji} \phi_i(n) + d_j(n), \quad T_L + T_{tr} + 1 \leq n \leq T, \quad 1 \leq j \leq r, \tag{10}$$

where the sequences $d_j(n) \triangleq v_j(n) + w_j(n)$, $1 \leq j \leq r$, account for the overall disturbance experienced during the payload phase. They still exhibit the *same* statistics previously detailed in (4),(5) are assumed independent from both path gains $\{h_{ji}\}$ and payload streams $\{\phi_j\}$. Therefore, after assuming that this last meets the (usual) power constraint

$$\frac{1}{t} \sum_{i=1}^t E\{|\phi_i(n)|^2\} = P, \quad T_L + T_{tr} + 1 \leq n \leq T \tag{10.1}$$

the resulting SINR γ_j measured at the output of the j-th receiving antenna during the payload phase equates² (see eqs.(5), (10))

$$\gamma_j = P/(N_0 + c_{jj}), \quad 1 \leq j \leq r. \tag{10.2}$$

Furthermore, from (10) we also deduce that column vector $\underline{y}(n) \triangleq [y_1(n) \dots y_r(n)]^T$ with r elements collecting the outputs of the r receiving antennas over n-th payload slot is linked to the (tx1) column vector $\underline{\phi}(n) \triangleq [\phi_1(n) \dots \phi_t(n)]^T$ of the corresponding signals radiated by Tx node as in

$$\underline{y}(n) = \frac{1}{\sqrt{t}} H^T \underline{\phi}(n) + \underline{d}(n), \quad T_L + T_{tr} + 1 \leq n \leq T, \tag{11}$$

² We point out that our model explicitly for the different power levels \tilde{P} and P possibly radiated by t transmitting antennas during training and payload phases respectively.

where $\{\underline{d}(n) \triangleq [d_1(n) \dots d_r(n)]^T, T_L + T_{tr} + 1 \leq n \leq T\}$ is the temporally white Gaussian sequence of the disturbance with spatial covariance matrix still given by K_d in (5). Furthermore, directly from (10.1) it follows that the t-tx spatial covariance matrix $R_\phi \triangleq E\{\underline{\phi}^\dagger \underline{\phi}\}$ of the t-dimensional signal radiated during each slot must meet the power constraint

$$Tra[R_\phi] \equiv E\{\underline{\phi}^\dagger \underline{\phi}\} = tP, T_L + T_{tr} + 1 \leq n \leq T. \quad (11.1)$$

Finally, after stacking the T_{pay} observed vectors in (11) into the corresponding $(T_{pay} \times 1)$ block vector $\underline{y} \triangleq [\underline{y}^T (T_L + T_{tr} + 1) \dots \underline{y}^T (T)]^T$, we may compact the T_{pay} relationship (11) in the following one:

$$\underline{y} = \frac{1}{\sqrt{t}} [I_{T_{pay}} \otimes H]^T \underline{\varphi} + \underline{d} \quad (12)$$

where the (block) covariance matrix of the corresponding disturbance block vector $\underline{d} \triangleq [\underline{d}^T (T_L + T_{tr} + 1) \dots \underline{d}^T (T)]^T$, equates

$$E\{\underline{d} (\underline{d})^\dagger\} = I_{T_{pay}} \otimes K_d \quad (12.1)$$

while the block vector $\underline{\phi} \triangleq [\underline{\phi}^T (T_L + T_{tr} + 1) \dots \underline{\phi}^T (T)]^T$ of random signals transmitted during overall payload phase is constrained as in (see 11.1):

$$E\{\underline{\phi}^\dagger \underline{\phi}\} = T_{pay} tP. \quad (12.2)$$

3 MMSE MIMO Channel Estimation in the Presence of Spatially Colored MUI

Since in [9] it is proved that the MMSE estimates $\hat{H} \equiv [\hat{h}_1 \dots \hat{h}_r] \triangleq E\{H|\tilde{Y}\}$ of the MIMO channel H in (9) is a *sufficient statistic* for the ML detection $\hat{\mathfrak{M}}$ of the transmitted message \mathfrak{M} , no information loss is paid by the here considered receiving architecture that it is composed by a MIMO MMSE channel-estimator cascaded to an ML detector of the transmitted message \mathfrak{M} . A suitable application of the Principle of Orthogonality leads to the following expression for the MMSE estimates $\hat{H}_j \triangleq E\{\hat{h}_j|\tilde{Y}\}$ of the j-th column of matrix H when both \tilde{Y} and the transmitted pilot matrix \tilde{X} are optimally employed at the receiver side:

$$\hat{h}_j = \frac{1}{\sqrt{t}} \left[\underline{e}_j^T K_d^{-1/2} \otimes \tilde{X}^\dagger \right] \left[\frac{1}{t} \left(K_d^{-1} \otimes \tilde{X} \tilde{X}^\dagger \right) + I_{rT_{tr}} \right]^{-1} \left(K_d^{-1/2} \otimes I_{T_{tr}} \right) vect(\tilde{Y}), \quad 1 \leq j \leq r \quad (13)$$

where r-dimensional (column) vector \underline{e}_j is the (usual) j-th unit vector of \mathbb{R}^r [13], $K_d^{-1/2}$ indicates the positive square root of matrix K_d^{-1} [13] while $vect(\tilde{Y})$ is the rT_{tr} -dimensional column vector given by the ordered stacking of the columns

observed matrix \tilde{Y} in (9). Furthermore, the cross-correlation matrices of the columns of the resulting MMSE error matrix $\mathfrak{E} \equiv [\underline{\varepsilon}_1 \dots \underline{\varepsilon}_1] \triangleq H - \hat{H}$ are given by

$$E \left\{ \underline{\varepsilon}_j (\underline{\varepsilon}_i)^\dagger \right\} = \delta(j, i) I_t - \frac{1}{t} (\underline{e}_j \otimes I_t)^\dagger \left(K_d^{-1/2} \otimes \tilde{X} \right)^\dagger \left[\frac{1}{t} \left(K_d^{-1} \otimes \tilde{X} \tilde{X}^\dagger + I_{rT_{tr}} \right) \right]^{-1} \cdot \left(K_d^{-1/2} \otimes \tilde{X} \right) (\underline{e}_i \otimes I_t), 1 \leq j, i \leq r \quad (14)$$

so that the resulting total mean square error $\sum_{tot}(\tilde{x}) \triangleq \|\mathfrak{E}\|_E^2$ equates (see (14) for $j=i$)

$$\begin{aligned} \sum_{tot} &= \sum_{j=1}^r Tra [\underline{\varepsilon}_j \underline{\varepsilon}_j^\dagger] = rt + \\ &- \frac{1}{t} \sum_{j=1}^r Tra \left[(\underline{e}_j \otimes I_t)^\dagger \left(K_d^{-1/2} \otimes \tilde{X} \right)^\dagger \left[\frac{1}{t} \left(K_d^{-1} \otimes \tilde{X} \tilde{X}^\dagger \right) + I_{rT_{tr}} \right]^{-1} \cdot \right. \\ &\quad \left. \cdot \left(K_d^{-1/2} \otimes \tilde{X} \right) (\underline{e}_j \otimes I_t) \right] \end{aligned} \quad (15)$$

3.1 Condition for the Optimal Training

Since the total mean square error in (15) depends on the matrix \tilde{X} employed for the training, the key-problem becomes how to choose \tilde{X} do to minimize (15) under power constraint (9.1). By fact, an application of Cauchy inequality [13] leads to the following condition characterizing optimal \tilde{X} .

Proposition 1. A training matrix \tilde{X} minimizes the total squared error (15) under power constraint (9.1) if and only if it meets the following relationship

$$K_d^{-1} \otimes \tilde{X}^\dagger \tilde{X} = a I_{rt} \quad (16)$$

where the positive scalar a equates

$$a \triangleq \frac{T_{tr} \tilde{P}}{r} Tra [K_d^{-1}] \quad \diamond (16.1)$$

4 Conveyed Information Throughput

The block-fading model introduced in Sect.II for the forward MIMO channel guarantees that this last is information stable [16] so that the corresponding Shannon's capacity C fixes the maximum information throughout conveyable in a reliable way during the payload phase. Following quite standard approaches [14], the capacity C of the MIMO channel (12) can be expressed as

$$C = \{C(\hat{H})\} \equiv \int C(\hat{H}) p(\hat{H}) d\hat{H}, \quad (\text{nats/payload slot}), \quad (17)$$

where the random variable

$$C(\hat{H}) \triangleq \sup_{\vec{\phi} : E\{\vec{\phi}^\dagger \vec{\phi}\} \leq t T_{pay} P} \frac{1}{T_{pay}} I(\vec{y}; \vec{\phi} | \hat{H}), \quad (18)$$

is the capacity of the MIMO channel (12), (12.2) *conditioned* on the realization \hat{H} of the channel estimates actually available at both transmitter and receiver. Finally, $I(\cdot; \cdot | \cdot)$ in (18) is the mutual information conveyed by the MIMO channel (12) during the payload phase. Unfortunately, barring two limit cases of PCSI [1,2,4,5] and NCSI [6,7], pdf of the input signals $\vec{\phi}$ achieving sup in (18) is currently *unknown* even for the simpler case of spatially white MUI. However, it is known that Gaussian distributed input signals achieve sup in (18) not only when condition of PCSI is approached [1,2,4,5] but also for $0 < \sigma_\varepsilon^2 < 1$ when length T_{pay} of the payload/phase (largely) exceeds number of t of transmit antennas (see [7] about this asymptotic important result). Therefore, motivated by above considerations, in the following we focus on the evaluation of (18) for Gaussian distributed input signals. In this case the T_{pay} components $\{\phi(n) \in \mathbb{C}^t, T_L + T_{tr} + 1 \leq n \leq T\}$ in (11) of the overall signal vector $\vec{\phi}$ in (12) are modeled as uncorrelated zero-mean proper complex Gaussian vectors with correlation matrix R_ϕ meeting (11.1). Obviously, the corresponding information throughput

$$C_G(\hat{H}) \triangleq \frac{1}{T_{pay}} \sup_{Tra[R_\phi] \leq Pt} I(\vec{y}; \vec{\phi} | \hat{H}) \quad (19)$$

conveyed by the MIMO channel (12) generally falls below $C(\hat{H})$ in (18), so that we have $C_G(\hat{H}) \leq C(\hat{H})$. However, above inequality is satisfied as equality when at least one of the above cited operating conditions is met. Therefore, passing now to deal with evaluation of $C_G(\hat{H})$ in (23), we have the following first property.

Proposition 2. Let us assume the training matrix \tilde{X} meeting the relationship (16) and also assigned the spatial correlation matrix R_ϕ in (11.1) of the payload streams radiated by t transmit antennas. Thus, the resulting conditional mutual information $I(\vec{y}; \vec{\phi} | \hat{H})$ in (19) supported by the MIMO channel (12) admits the following closed-form expression:

$$I(\vec{y}; \vec{\phi} | \hat{H}) = T_{pay} \lg \det \left[\left(I_r + \frac{1}{t} K_d^{-1/2} \hat{H}^T R_\phi \hat{H}^* K_d^{-1/2} + \sigma_\varepsilon^2 P K_d^{-1} \right) \cdot \left(I_{rt} + \frac{\sigma_\varepsilon^2 T_{pay}}{t} (K_d^{-1}) \otimes R_\phi \right)^{-1/T_{pay}} \right] \quad (20)$$

when at least one of the conditions below listed is met:

a) both T_{pay} and t are large; (20.1)

b) σ_ε^2 vanishes; (20.2)

c) all SINRs γ_j , $1 \leq j \leq r$, in (10.2) vanish. \diamond (20.3)

4.1 Optimized Power Allocation in the Presence of Colored MUI

Therefore, according to (19), we must proceed to the power-constrained maximization of conditional throughput (20). For this purpose, first let us indicate as

$$K_d = U_D \Lambda_D U_D^\dagger, \tag{21}$$

the Singular Value Decomposition (SVD) of MUI spatial covariance matrix K_d , with

$$\Lambda_D \triangleq \text{diag}\{\mu_1, \dots, \mu_r\} \tag{21.1}$$

indicating the corresponding (rxr) diagonal matrix of the *magnitude-ordered* singular values. Second, after introducing the (txr) matrix

$$A \triangleq \hat{H}^* K_d^{-1/2} U_D, \tag{22}$$

accounting for the *combined* effects of imperfect channel estimates \hat{H} and MUI spatial coloration K_d , let us denote as

$$A = U_A D_A V_A^\dagger \tag{22.1}$$

the related SVD, where U_A and V_A are unitary matrices, while

$$D_A \triangleq \text{diag}\{K_1, \dots, K_s, \mathbf{0}_{t-s}\}, \tag{22.2}$$

is the corresponding (txr) diagonal matrix collecting the $s \triangleq \min\{r, t\}$ *magnitude-ordered* singular-values $k_1 \geq k_2 \geq \dots \geq k_s > 0$ of matrix A. Finally, for future convenience, let us also introduce the following dummy positions:

$$\alpha_m \triangleq \frac{\mu_m k_m^2}{t(\mu_m + P\sigma_\varepsilon^2)}, \quad 1 \leq m \leq s; \quad \beta_l \triangleq \frac{\sigma_\varepsilon^2 T_{pay}}{t\mu_l}, \quad 1 \leq l \leq r. \tag{23}$$

Thus, the application of the Kuhn-Tucker conditions [14, eqs.(4.4.10), (4.4.11)] allows us to evaluate the optimized transmit powers $\{P^*(m), 1 \leq m \leq t\}$ achieving the constrained sup in (19) as detailed in the following proposition.

Proposition 3

Let us assume that at least one of the above operating conditions (20.1), (20.2), (20.3) is fulfilled. Thus, for $m = s + 1, \dots, t$, the powers achieving sup in (19) *vanish* while for $m = 1, \dots, s$ they are computed according to the following two relationship

$$P^*(m) = 0, \text{ when } k_m^2 \leq \left(1 + \frac{\sigma_\varepsilon^2 P}{\mu_m}\right) \left(\frac{t}{\rho} + \sigma_\varepsilon^2 \text{Tra}[K_d^{-1}]\right), \tag{24}$$

$$P^*(m) = \frac{1}{2\beta_{min}} \left\{ \beta_{min} \left[\left(1 - \frac{r}{T_{pay}}\right) \rho - \frac{1}{\alpha_m} \right] - 1 + \right.$$

$$+ \sqrt{\{\beta_{min} \left[\left(1 - \frac{r}{T_{pay}}\right) \rho - \frac{1}{\alpha_m} \right] - 1\}^2 + 4\beta_{min} \left(\rho - \frac{1}{\alpha_m} - \frac{r\rho\beta_{min}}{\alpha_m T_{pay}} \right)\}},$$

when

$$k_m^2 > \left(1 + \frac{\sigma_\varepsilon^2 P}{\mu_m}\right) \left(\frac{t}{\rho} + \sigma_\varepsilon^2 \text{Tra}[K_d^{-1}]\right). \quad (25)$$

Furthermore, the nonnegative scalar parameter ρ in (24), (25) is set so to satisfy the power constraint (see eq.(11.1))

$$\sum_{m \in \mathcal{J}(\rho)} P^*(m) = Pt, \quad (26)$$

where

$$\mathcal{J}(\rho) \triangleq \{m = 1, \dots, s : k_m^2 > \left(1 + \frac{\sigma_\varepsilon^2 P}{\mu_m}\right) \left(\frac{t}{\rho} + \sigma_\varepsilon^2 \text{Tra}[K_d^{-1}]\right)\}, \quad (26.1)$$

is the (ρ -depending) indexes set fulfilling inequality (25). Finally, the corresponding optimized spatial correlation matrix for the radiated signals is aligned along right-eigenvectors of matrix A in (22.1) according to

$$R_\phi(\text{opt}) = U_A \text{diag}\{P^*(1), \dots, P^*(s), \mathbf{0}_{t-s}\} U_A^\dagger, \quad (27)$$

so that the resulting maximized throughput in (19) admits the following (simple) closed-form expression:

$$C_G(\hat{H}) = \sum_{m=1}^r \left(1 + \frac{\sigma_\varepsilon^2}{P} \mu_m\right) + \sum_{m=1}^s \left[\lg(1 + \alpha_m P^*(m)) - \frac{1}{T_{pay}} \sum_{l=1}^r \lg(1 + \beta_l P^*(m)) \right] \diamond \quad (28)$$

About above reported power allocation, some remarks are in order. First, an exploitation of the (truncated) expansion: $\sqrt{1+x} \approx 1 + 0.5x$ allows us to rewrite (24), (25) in the following form for vanishing σ_ε^2 :

$$\lim_{\sigma_\varepsilon^2 \rightarrow 0} P^*(m) = \max \left\{ 0, \rho - \frac{t}{k_m^2} \right\}, \quad m = 1, \dots, s, \quad (29)$$

and this last agrees with the water-filling like power allocation previously reported in [1,2] for the case of *perfect* channel estimation. Second, when σ_ε^2 approaches unit then channel estimates \hat{H} vanish so that no information is available at both transmit and receiver about actual values assumed by MIMO channel path gains $\{h_{ji}\}$. In this limit case, we arrive at the following limit expression for the sustained throughput $C_G(\hat{H})$ in (19):

$$\lim_{\sigma_\varepsilon^2 \rightarrow 1} C_G(\hat{H}) \triangleq C_G(0) = \sum_{m=1}^r \lg \left[\frac{\left(1 + \frac{P}{\mu_m}\right)}{\left(1 + \frac{T_{pay}}{\mu_m}\right)^{1/T_{pay}}} \right], \quad (\text{nats/payload slot}) \quad (30)$$

Since this last holds for large t and T_{pay} regardless of radiated power P , relationship (30) directly *supports* the conjecture originally reported in [7] about the capacity-achieving property retained for *large* T_{pay} by the input Gaussian pdf *even* in application scenarios with non-coherent detection.

4.2 A Numerical Algorithm for Implementing the Optimized Power Allocation

Passing now to shortly consider numerical implementation of presented Power Allocation formulas, the first step for computing (24), (25) relies on evaluating ρ value satisfying relationship (26). Although this computation resists closed-form analytical evaluation in the simpler case of PCSI [1,2], nevertheless we observe that cardinality $|\mathcal{J}(\rho)|$ of the indexes' set in (26.1) vanishes at $\rho = 0$ and then increases for growing ρ . This means that the solution of (26) may be found by implementing a (very) simple iterative procedure that starts with $\rho = 0$ and then progressively increases the current value of ρ by a pre-assigned step-size Δ until summation in (26) equates the power constraint Pt . The resulting algorithm for the numerical evaluation of the optimized powers (24), (25) is summarized in Table I and several performance plots obtained via its computer-implementation will be presented in Sect.VI.

Table 1. Pseudo-code for a numerical implementation of the optimized power allocation algorithm.

1. Compute and order eigenvalues of MUI covariance matrix \bar{K}_d ;
2. Compute SBD of matrix A in (22.1) and order its singular values;
3. Set $P^*(m) = 0$, $1 \leq m \leq t$;
4. Set $\rho = 0$ and $\mathcal{J}(\rho) = \emptyset$;
5. Set step size Δ ;
6. While $\left(\sum_{m \in \mathcal{J}(\rho)} P^*(m) < Pt \right)$ do
 7. Update $\rho = \rho + \Delta$;
 8. Update set $\mathcal{J}(\rho)$ via eq. (26.1);
 9. Compute powers set $\{P^*(m), m \in \mathcal{J}(\rho)\}$;
10. end;
11. Compute optimized powers $\{P^*(m), 1 \leq m \leq s\}$ via eqs. (24), (25);
12. Compute optimized shaping matrix $R_\phi(opt.)$ via eq.(27);
13. Compute conveyed throughput $C_G(\hat{H})$ via eq.(28);

5 Numerical Results and Performance Comparisons

Although joined pdf of the (rxt) elements of the channel estimates \hat{H} is known [9], nevertheless the corresponding expectation

$$C_G \triangleq E\{C_G(\hat{H})\}, \quad (31)$$

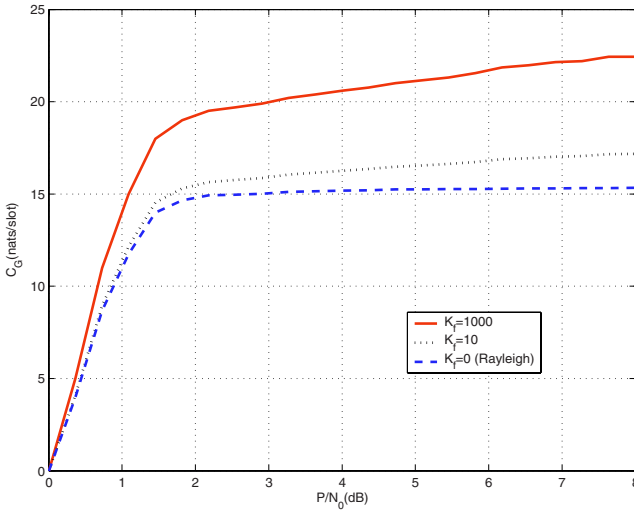


Fig. 1. Sensitivity of the Throughput C_G conveyed by the reference link Tx0 \rightarrow Rx0 on the Ricean Factor k in (38) for $T_{pay} = 80$, $r=t=10$, $\sigma_\varepsilon^2 = 0.1$).

of the conditional throughput in (28) resists closed-form analytical evaluation even in the simplest case of spatially white MUI with vanishing σ_ε^2 [4,5,17 and reference therein]. Thus, as in [1,2,4] in this Section we resort to a Monte-Carlo approach for computing expectation based on sample-average of 10,000 independent realizations of conditional throughput $C_G(\hat{H})$. Furthermore, all the reported numerical plots refer to a hexagonal network with N_0 set to unit and various values of the power level P radiated by transmit nodes. Plots of Fig.1 allow us to appreciate the effect of the Ricean Factor k_f on the average throughput conveyed by the reference link for $T_{pay} = 80$, $r=t=10$ and $\sigma_\varepsilon^2 = 0.1$. From these last plots we conclude that when interference presents Rayleigh features the system performances fall short. Although in these years MAI-mitigation capability offered by multi-antenna systems based on smart-like technology has been often claimed [8,15,18], nevertheless a still open question concerns comparison of information throughputs C_G conveyed by here considered MAI-impaired systems with those guaranteed by orthogonal MAI-free TDMA (or FDMA) based access techniques.

By fact, till now no firm evidence of superiority of an access technique over the other one is available in the literature, specially for the application scenarios here considered where typical SINRs values are of the order of few dBs so that multiuser detection strategies based on iterative subtractive cancellations of MAI tend to fall short [22]. To gain some (preliminary) insight about this important question, we have numerically evaluated the average information throughput $C_{TDMA} = E\{C_{TDMA}(\hat{H})\}$ (nats/ payload slot) conveyed by the reference link when a MAI-free TDMA-based access is implemented.

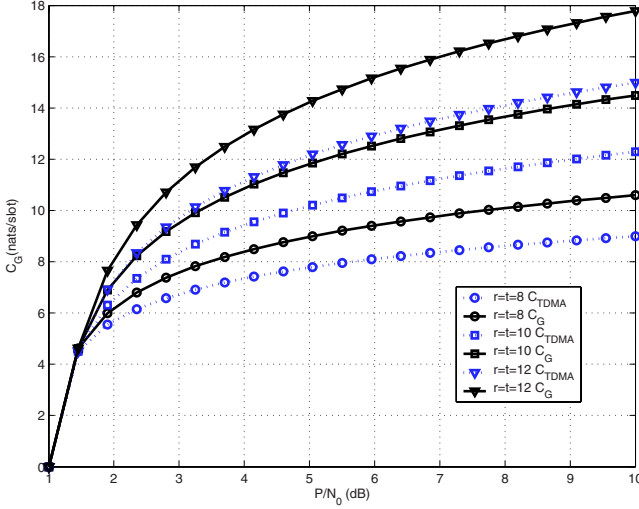


Fig. 2. C_{TDMA} throughput comparisons for the reference link Tx0 \rightarrow Rx0 for $T_{pay} = 80$, $k=1000$, $\sigma_\varepsilon^2 = 0.1$).

The obtained numerical plots of Fig.2 refer to the network with $T_{pay} = 80$, $\sigma_\varepsilon^2 = 0.1$, $k = 1000$ and values of number of transmit/receiving antennas ranging from 4 to 12. Although C_G has been evaluated in the worst-MAI condition, nevertheless plots of Fig.2 show that C_G outperforms corresponding C_{TDMA} , specially at low radiated power level P and for transceivers equipped with large number $r=t$ of transmit/receiving antennas. Thus, we may conclude that when r and t increase the proposed spatial shaper allows us to achieve Channel Capacity that is higher than the one achieved by orthogonal access methods.

6 MAC Implications and Conclusions

The underlying conclusion seems to be that allowing multiple users to collide in the time-frequency plan leads to a more effective utilization of the spatial dimension of the receivers that, by fact, over-compensates throughput loss induced by collisions experienced in the time-frequency domain. Based on this conclusion, a more effective MAC strategy may be to allow for some forms of hybrid multi-access scheme where (a moderate level of) collisions are tolerable in the time-frequency domain so to fully exploit the space-division access capability of the multi-antenna system. An example of non-orthogonal access technique may be OFDMA with *tone-sharing* among multiple users, where the degree of tone-sharing increases with the number of transmit/receive antennas. This conclusion demands for new MAC paradigm and related MAC design criteria where the spatial MAC capability of the Multi-Antenna system is carefully exploited.

References

1. F.R. Farrokhi, G.J. Foschini, A. Lozano, R.A. Valenzuela, "Link-Optimal BLAST processing with Multiple-Access Interference", VTC2002, pp.87–91.
2. F.R. Farrokhi, G.J. Foschini, A. Lozano, R.A. Valenzuela, "Link-Optimal Space-Time Processing with Multipole Transmit and Recieve Antennas", IEEE Comm. Letters, vol.5, no.3, pp.85–87, March 2001.
3. S.L. Marple Jr., Digital Spectral Analysis with Applications, Prentice Hall, 1987.
4. C.-N. Chuan, N.D.S. Tse, J.M. Kahn, R.A. Valenzuela, "Capacity-scaling in MIMO wireless Systems under correlated Fading", IEEE Trans. on Inform. Theory, vol.48, no.3, pp.637–650, March 2002.
5. G.J. Foschini, M.J. Gans, "On limit of wireless communicqations in fading environment when using multiple antennas", Wireless Pers. Comm., vol.6, no.3, pp.311–325, June 1998.
6. B. Hassibi, T.L. Marzetta, "Multiple-Antennas and Isotropically Random Unitary Inputs: the received Signal Density in closed form", IEEE Trans. on Infrom. Theory, vol.48, no.6, pp.1473–1485, June 2002.
7. T.L. Marzetta, B.M. Hochwald, "Capacity of a mobile Multiple-Antenna Communication link in Rayleigh flat fading", IEEE Trans. on Inform. Theory, vol.45, no.1, pp.139–157, January 1999.
8. R.D. Murch, K.B. Letaief, "Antenna System for broadband Wireless Access", IEEE Comm. Mag., pp.637–650, March 2002.
9. J.-C. Guey, M.P. Fitz, M.R. Bell, W.-Y. Kuo, "Signal Design for Transmitter Diversity Wireless Communication System Over Rayleigh Glat fading channels", IEEE Trans. on Comm., vol.47, no.4, pp.527–537, April 1999.
10. J. Baltarsee, G. Fock, H. Meyr, "Achievable Rate of MIMOChannels with data-aided channel-estimation and perfect interleaving", IEEE Journ. on Selected Areas in Comm., vol.19, no.12, pp.2358–2368, Dec.2001.
11. E. Baccarelli, M. Biagi, A. Fasano, "Optimized Design and Performance of Multiple-Antenna 4th Generation WLANs for Partially-Coherent Decoding", European Wireless 2002 Conference Proceedingd, Florence 25–28 February 2002, vol2, pp.858–864
12. T.M. Cover, J.A. Thomas, Elements of Information Theory, Wiley, 1991.
13. P. Lancaster, M. Tismetesky, The theory of Matrices, 2nd Ed., Academic press, 1985.
14. R.G. Gallager, Information heory and Reliable Communication, Wiley, 1968.
15. G.T. Okamoto, Smart Antennas Systems and Wireless LANs, kluwert 2001.
16. S. Verdú, T.S. Han, "A general Formula for channel Capacity", IEEE Trans. on Inform. Theory, vol.40, no.6, pp.1147–1157, July 1994.
17. D.W. Bliss, K.W. Forsythe, A.O. Hero, A.F. Yegulalp, "Environmental Issues for MIMO Capacity", IEEE Trans. on Signal Proc., vol.50, no.9, pp.2128–2142, Sept. 2002.
18. A. Santamaria, F.J. L.-Hernandez, Wireless LAN Standards and Applications, Artech House, 2001.
19. H. Sampath, S. Talwar, J. Tellado, V. Erceg, A. Paulraj, "A 4th Generation MIMO-OFDM Broadband Wireless System: Design, Performance and Field Trials results", IEEE Comm.Mag., pp.143–149, Sept.2002.
20. C.E. Perkins, Ad Hoc Networking, Addison Wesley, 2000.
21. E. Baccarelli, M. Biagi, "Error Resistant Space-Time Coding for Emerging 4G-WLANs", presented at Wireless Communication and Networking Conference (WCNC) 2003, 16–20 March 2003, New Orleans, Lousiana, U.S.A.

22. S. Verdú, *Multuser Detection*, Cambridge Uni. Press, 1998.
23. A. Lozano, A.M. Tulino, "Capacity of Multiple-Transmit Multiple-Receive Antenna Architecture", *IEEE Trans. on Inform. Theory*, vol.48, no.12, pp.3117–3128, Dec.2002.
24. E. Baccarelli, M. Biagi, "A New Family of Space-Time Codes for Multi-Antenna Systems with Imperfect Channel Estimation", (INVITED PAPER), *IEEE International Symposium on Advances in Wireless Communications (ISWC'02)* conference proceedings, Victoria, BC, Canada September 23–24, pp.83–84.